Mixtures of an Acid-Functionalized Mesogen with Poly(4-vinylpyridine)

Frank A. Brandys and C. Geraldine Bazuin*

Centre de recherche en sciences et ingénierie des macromolécules (CERSIM), Département de chimie, Université Laval, Québec, Canada G1K 7P4

Received June 2, 1995[⊗]

A thermotropic dialkoxy biphenyl liquid crystal, functionalized by a carboxylic acid group at one extremity, is mixed to varying proportions with poly(4-vinylpyridine) (P4VP). The liquid crystal, LC-4,6A, is characterized by a monotropic smectic A phase and a highly ordered or crystalline lamellar phase formed primarily of acid dimers. In the mixtures with P4VP (studied up to acid/pyridine molar ratios of 1.0), the fluid mesophase is suppressed. A solid−isotropic phase transition is present above a molar ratio of about 0.2, whereas for lower LC-4,6A contents the mixtures form an apparently miscible, amorphous material. The glass transition temperature, T_g, of the latter is strongly depressed, at a rate of 7 °C/mol % LC-4,6A up to a molar ratio of 0.1, after which the T_g remains essentially constant. As supported by infrared analysis, the plasticization behavior is attributed to strong hydrogen bonding between the acid and pyridine moieties, which solubilizes the LC-4,6A molecules within the polymer matrix. When the solubility limit is reached, the excess small molecule solidifies into an ordered phase that is essentially identical to that of neat LC-4,6A. This phase can be modified by quenching from the melt, which freezes in a greater proportion of the acid−pyridine interactions and leads to incorporation into this phase of significant amounts of P4VP.

Introduction

A new family of polymeric liquid-crystalline materials, based on the use of strong noncovalent interactions between constituent components, is undergoing exploration in several laboratories. The electrostatic interactions utilized are based primarily on hydrogen bonding[1−5] or ion−ion bonding.[2,6] The resulting materials can self-assemble into both side-chain-like[1,2,5,6] and main-chain-like[3,4] polymers.

Intermolecular hydrogen bonding is frequently achieved using carboxylic (or benzoic) acid and pyridine (or pyridyl) moieties. The Kato and Fréchet team, in particular, have investigated a variety of side-chain-like hydrogen-bonded complexes based on benzoic acid−pyridyl interactions. The benzoic acid group is part of the polymer side chain and is separated from the main chain (polyacrylate[1] and polysiloxane[7]) by an alkyl spacer. This polymer is blended with rigid molecules such as stilbazole and its derivatives. The hydrogen bond which complexes the acid (donor) and pyridyl (acceptor) groups becomes part of the rigid core of the mesogenic unit in the complex and thereby contributes to extending the original core. Depending on the particular constituents involved (which include bifunctional small molecules), various liquid-crystalline phases are obtained, or stabilized, including nematic and smectics A, B, and C (the constituents separately are also frequently liquid crystalline, although this is not a necessary condition[7]). Ferroelectric properties were also successfully induced in such a system, through the use of a chiral stilbazole derivative.[8] In all of the systems studied by Kato, Fréchet, and co-workers, acid−pyridine complexation is thermodynamically favored over acid dimerization.

Griffin and co-workers[4] also complexed benzoic acid and pyridine moieties, in their case using bifunctional small molecule constituents in order to form main-chain-like liquid-crystalline polymers. A particularly elegant main-chain-like system was assembled by Lehn and co-workers;[3] it involves triply hydrogen-bonded complexes of chiral constituents, resulting in hexagonal columnar mesophases having a triple-helical superstructure. Finally, in a very recent report,[5] it is claimed that (side-chain-like) liquid-crystalline polymeric materials can be produced from hydrogen-bonded nonmesogenic constituents composed of functional vinyl polymers and rigid, aromatic derivatives without the presence of a spacer chain; in other words, the hydrogen bond is located near the polymer main chain.

In this paper, we present results obtained for a functional polymer−small molecule system, potentially mimicking side-chain polymer architecture, where the hydrogen bonds that take place are located near the polymer main chain and where an alkyl spacer is

[⊗] Abstract published in *Advance ACS Abstracts,* September 1, 1995.

(1) (a) Kato, T.; Fréchet , J. M. J. *Macromolecules* **1989**, *22*, 3819. (b) Kato, T.; Kihara, H.; Uryu, T.; Fujishima, A.; Fréchet, J. M. J. *Macromolecules* **1992**, *25*, 6836. (c) Kato, T.; Kihara, H.; Kumar, U.; Uryu, T.; Fréchet, J. M. J. *Angew. Chem., Int. Ed. Engl.* **1994**, *33*, 1644.

(2) Bazuin, C. G.; Brandys, F. A.; Eve, T. M.; Plante, M. *Makromol. Chem., Macromol. Symp.* **1994**, *84*, 183.

(3) Lehn, J.-M. *Angew. Chem., Int. Ed. Engl.* **1990**, *29*, 1304.

(4) (a) Alexander, C.; Jariwala, C. P.; Lee, C.-M.; Griffin, A. C. *Am. Chem. Soc., Polym. Prepr.* **1993**, *34*, 168. (b) Bladon, P.; Griffin, A. C. *Macromolecules* **1993**, *26*, 6604.

(5) Malik, S.; Dhal, P. K.; Mashelkar, R. A. *Macromolecules* **1995**, *28*, 2159.

(6) Ujiie, S.; Iimura, K. *Macromolecules* **1992**, *25*, 3174.

(7) Kumar, U.; Kato, T.; Fréchet, J. M. J. *J. Am. Chem. Soc.* **1992**, *114*, 6630.

(8) Kumar, U.; Fréchet, J. M. J.; Kato, T.; Ujiie, S.; Iimura, K. *Angew. Chem., Int. Ed. Engl.* **1992**, *31*, 1531.

0897-4756/96/2808-0083$12.00/0

present as part of the small molecule constituent. The polymer, poly(4-vinylpyridine) (P4VP), is easy to synthesize (and is commercially available). The mesogenic small molecule is a dialkoxy biphenyl, where one of the alkyl chains is end-functionalized with carboxylic acid. The chemical structures of the two constituents are illustrated in **1** in their hydrogen-bonded form. The mesogen will be referred to as LC-4,6A, where the numbers tally the carbon atoms in each alkyl chain, and A indicates that the functional end group of the 6-carbon spacer is acidic.

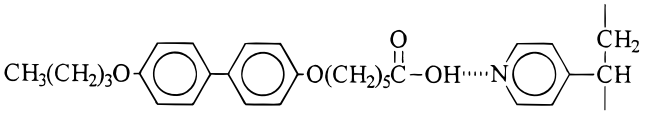

1

Experimental Section

Synthesis. The functionalized mesogen, LC-4,6A, was prepared in two steps, using standard procedures for Williamson ether synthesis. The starting reactant, 4,4′-biphenol (97%, Aldrich), was neutralized with 2 equiv of KOH (reagent, Baker) in dry methanol (0.1 M solution). During refluxing of the solution, 1 equiv of 1-bromobutane (99%, Aldrich) was added dropwise, and refluxing was continued for 4 h. The major monosubstituted and minor bisubstituted products precipitated during that time and were collected after cooling of the mixture to room temperature. The filtrate was washed with dry methanol and then added to 0.1 M aqueous HCl, upon which an emulsion was formed. The emulsion was stirred for 30 min and then filtered and washed with water. The resulting white paste was dried and then dissolved in hot ethanol (99.5%), hot-filtered (this step removes any bisubstituted product present), and recrystallized twice (yield 65%).

In the second step, 2 equiv of sodium (3−8 mm spheres, Aldrich) was dissolved into 99.5% ethanol, to give a 0.1 M solution. The monosubstituted product was added, and a clear, colorless solution was obtained on refluxing. An equivalent of 6-bromohexanoic acid (98%, Aldrich) was dissolved separately in 99.5% ethanol (1 M solution) and then added all at once to the refluxing solution. After overnight refluxing, the mixture was reduced to a quarter of its volume, and the resulting precipitate was collected and washed with 99.5% ethanol. Once dry, the final product was acidified as above, allowed to stir for 30 min, filtered, washed with water, and recrystallized twice from chloroform (yield 75%). NMR (Bruker, 300 MHz, ^{1}H, $CDCl_3$) $\delta = 7.46$ (4H, d, $J = 9$, Ar), 6.94 (4H, d, $J = 9$, Ar), 3.99 (4H, t, $J = 8$, OCH_2), 2.41 (2H, t, $J = 7$, CH_2 acid), 1.79 (6H, m, $J = 7$, CH_2), 1.54 (4H, m, $J = 7$, CH_2), 0.99 (3H, t, $J = 7$, CH_3). Thermogravimetric analysis (Mettler TGA-50, 10 °C/min) of the product indicated that it is stable in air to well over 200 °C; furthermore, there was less than 1% weight loss for a 20-min isothermal run at 180 °C, about 2% at 200 °C.

Poly(4-vinylpyridine) was polymerized by free-radical procedures at 70 °C in dry methanol for 12 h, using AIBN (obtained from Prof. G. Darling, McGill University) as the initiator. The degree of conversion was 47%. The polymer was purified by precipitating twice into hexanes from a 1 M methanol solution of P4VP. To facilitate the preparation of the mixtures, the polymer was freeze-dried from a 0.1 M 80/20 (v/v) benzene/methanol solution and dried under reduced pressure for 2 weeks at 90 °C (yielding a tan-colored fluff). The infrared spectrum for the product is identical to that published in ref 9 and to a commercial P4VP (Scientific Polymer Products), and the glass transition temperature is comparable to that reported in refs 9 and 10.

Mixtures of LC-4,6A and P4VP were prepared by dissolving the two components separately to make 0.1 M 80/20 (v/v) benzene/methanol solutions; these solutions were mixed and then stirred for 12 h. Finally, the mixtures were freeze-dried and further dried under vacuum at 90 °C for several days. The dried mixtures were white, with a cotton-like appearance. In earlier work, the components were dissolved in $CHCl_3$, and the solvent was evaporated after cooling the solution in Petri dishes. No notable differences in the subsequent analyses were observed between the methods of preparation. The freeze-drying method was chosen in order to facilitate drying and the preparation of larger batches and was necessary for solid-state NMR measurements (to be published separately[11]). The compositions of the mixtures are generally described in terms of the molar ratio of acid to pyridine units or, in other words, of liquid-crystalline molecules to P4VP repeat units (LC-4,6A:P4VP).

Analyses. Differential scanning calorimetry (DSC) thermograms were obtained with a Perkin-Elmer DSC-4 and a Mettler DSC-20, calibrated with indium. The scans were performed at either 5 or 20 °C/min, depending on whether first-order transitions or the glass transition temperature were being analyzed. Samples ranged in weight from around 5−12 mg for samples of acid:pyridine molar ratios greater than 0.2 to about 15−23 mg for samples of lower molar ratios. The samples were initially melted and maintained at about 170 °C for 5 min, then either cooled slowly at −5 °C/min (unless otherwise specified) or quenched at a nominal speed of −320 °C/min prior to the heating scans. The first-order transition temperatures are given as the maxima or the minima, and the glass transition temperature as the midpoint of the transitions. The transitions were constant in multiple scans.

Observations of the transitions and textures were made using a Zeiss Axioskop polarizing optical microscope equipped with a Leica (UT40/0.34) objective. The temperature was regulated with a Mettler FP5 temperature controller and Mettler FP52 hot stage.

Infrared spectra were obtained from an accumulation of 100 scans at a resolution of 2 cm^{-1} using a Mattson Sirius 100 spectrometer equipped with an MCT detector. Unless otherwise specified, the spectra were taken at ambient temperature of samples ground in dry KBr (FTIR grade, Aldrich) and molded into pellets. For scans involving quenched samples, the KBr pellets were preheated to above the sample melting point, using the Mettler FP52 hotstage, and then dropped into a double pan containing liquid nitrogen. In some cases, samples were cast from 80/20 (v/v) benzene/methanol or chloroform solutions onto KBr disks (Wilmad) and dried as described above. It was noted that some band intensities are sensitive to the method of preparation, although the main trends were the same.

X-ray diffractograms were obtained using a Rigaku Rotaflex RU-200BH rotating anode, with Ni-filtered Cu Kα radiation, operating at 55 kV/190 mA. At small angles (SAXS), the beam was collimated by successive slits having widths of 0.16 and 0.12 mm. A camera under vacuum was located between the samples and detector, with a 0.1-mm slit located just before the detector. At wide angles (WAXS), collimation was effected with a Soller slit and a 2 mm pinhole, giving an instrumental resolution of 1°. SAXS profiles were recorded at 0.1°(2θ)/min and WAXS profiles at 1°(2θ)/min, using SC-30 Rigaku scintillation counters coupled to pulse-height analyzers. In all cases, the samples were packed with a metal rod into 1.5-mm glass capillary tubes (Charles Supper) and sealed. A water-cooled oven, constructed in our laboratories, was used for the variable temperature runs. The temperature was stable to ±1 °C. Quenched samples, in capillary tubes, were prepared in the same manner as for the IR analyses. All profiles obtained were treated by subtracting a baseline profile obtained with an empty capillary tube, and most of the data obtained were smoothed.

Dynamic mechanical thermal analysis was performed with a MKII Polymer Laboratories DMTA in the bending mode at

(9) Huglin, M. B.; Rego, J. M. *Polymer* **1990**, *31*, 1269.

(10) Brandrup, J., Immergut, E. H., Eds. *Polymer Handbook*, 2nd ed.; Wiley: New York, 1975; Chapter III.

(11) In collaboration with A. Natansohn, Queen's University, Kingston; to be published.

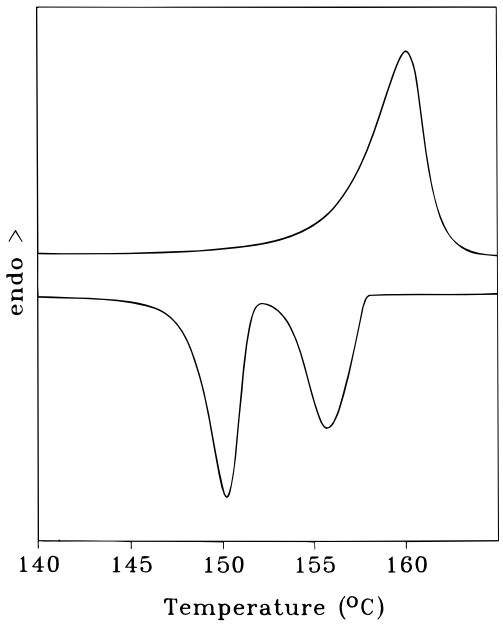

Figure 1. DSC thermograms (heating and cooling at 5 °C/min) of LC-4,6A.

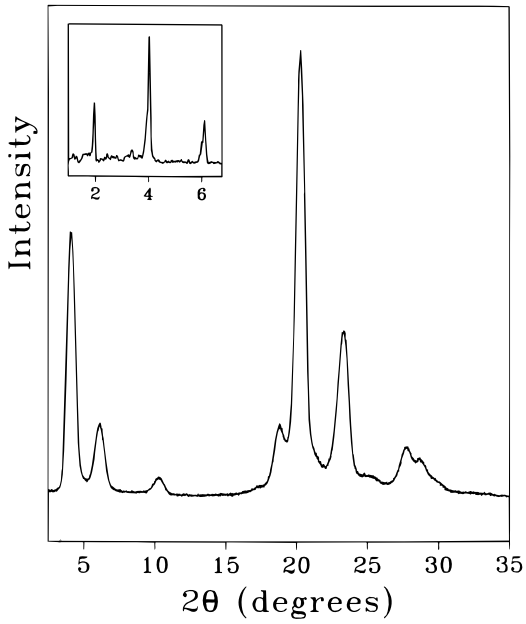

Figure 2. Ambient temperature X-ray profile of LC-4,6A. The inset shows the profile obtained with the small-angle camera.

a frequency of 0.3 Hz and a nominal deflection of 64 μm. Rectangular bars were compression-molded at about 20 °C above the glass transitions by applying 10 000 psi for 10 min. The samples were then cooled slowly to ambient temperature and placed overnight under reduced pressure at ambient temperature. The final sample dimensions were 2 × 8 × 25 mm, with 5 mm of free length between the clamps.

Results

Pure LC-4,6A. The mesogenic compound used is novel in that it possesses not only the usual flexible (alkyl chain) and rigid (biphenyl) moieties characteristic of low molar mass liquid crystals but also a polar head group located at the opposite end of one of the alkyl chains from the mesogen. These types of compounds are only recently receiving increased attention.[2,6,12−15]

The DSC traces (first cooling and second heating at 5 °C/min) for the compound are shown in Figure 1. A single transition with a maximum at 160 °C (enthalpy 32 kJ/mol) is observed on heating, whereas two transitions with their minima at 156 °C (enthalpy 14 kJ/mol) and 150 °C (enthalpy 18 kJ/mol) are observed in the cooling curves.[16] The transition temperatures were confirmed by polarizing optical microscopy. On cooling from the melt, golden batonnets form at the higher temperature transition and develop into a fluid, focal conic texture with homeotropic regions on further cooling. This texture is characteristic of a smectic A phase. Interestingly, the enthalpy of the S_A−I transition is an order of magnitude higher than usual; this is probably related to the hydrogen-bonding interactions among acid molecules. The lower temperature transition is marked by the growth of a colorful texture which tends to grow in as square-like and lathe-like patterns;[18] ghost-like textures were also observed in some areas where the sample was thin.

X-ray diffractograms[19] are consistent with the smectic A assignment of the high-temperature mesophase: a broad peak centered at about $2\theta = 20°$, typical of disordered alkyl chains and corresponding to a Bragg spacing of about 4.5 Å, is accompanied by a single sharp diffraction peak at $2\theta = 3.7°$, corresponding to a Bragg spacing of 23 Å. The molecular length of LC-4,6A in its most extended conformation is about 25 Å [modeled using the Alchemy software (Tripos) and taking into account the van der Waal's radius at the extremities]. Clearly, the LC-4,6A molecules are arranged in single layers, with their molecular axis perpendicular on average to the layer planes. Any H-bonding interactions (between layers) which may take place in this fluid phase are necessarily labile.

The diffractogram of the lower temperature phase (Figure 2) is typical of a crystalline or highly ordered, lamellar phase. At small angles, a series of sharp diffraction peaks, with reciprocal spacings in the ratio 1:2:3 (and, apparently, :5), are observed. All of these peaks increase slightly in 2θ with increasing temperature (about 5% over the entire range). The lowest angle peak, at $2\theta = 2.0°$, corresponds to a Bragg spacing of 44 Å. This indicates that the molecules are arranged in orthogonal bilayers, most likely in the form of acid dimers as will be confirmed by infrared spectroscopy (see later). The formation of acid dimers can also account for the bilayer thickness being somewhat less than twice the monolayer thickness. At wide angles,

(12) Navarro-Rodriguez, D.; Frère, Y.; Gramain, Ph.; Guillon, D.; Skoulios, A. *Liq. Cryst.* **1991**, *9*, 321.
(13) Fuller, S.; Hopwood, J.; Rahman, A.; Shinde, N.; Tiddy, G. J.; Attard, G. S.; Howell, O.; Sproston, S. *Liq. Cryst.* **1992**, *12*, 521.
(14) Chien, L.-C.; Cada, L. G.; Xie, L. *Liq. Cryst.* **1992**, *12*, 853.
(15) Centore, R.; Roviello, A.; Sirigu, A. *Liq. Cryst.* **1989**, *6*, 175.
(16) DSC curves published earlier[17] for this compound were taken of samples thermally treated near 200 °C for 20 min, which apparently altered their polymorphism.
(17) (a) Bazuin, C. G.; Brandys, F. A. *Chem. Mater.* **1992**, *4*, 970. (b) Brandys, F. A.; Bazuin, C. G. *Am. Chem. Soc., Polym. Prepr.* **1993**, *34*, 186.
(18) The texture observed resembles a colorful version of plate 34, for a paramorphotic smectic E texture, in: Gray, G. W.; Goodby, J. W. G. *Smectic Liquid Crystals, Textures and Structures*; Leondard Hill: Glasgow, 1984.
(19) This result was obtained for us by R. Seghrouchni and A. Skoulios (see Acknowledgements) on a photographic plate using Cu $K\alpha_1$ radiation and a vacuum Guinier focusing camera equipped with a bent-quartz monochromator; this was confirmed by them in a 1-min exposure time during which the X-ray profile was recorded with the Inel CPS120 curved position-sensitive detector.

two sharp peaks are observed, with their maxima at 20.0° and 22.2° (2θ) for temperatures near 100 °C (corresponding to Bragg spacings of 4.4 and 4.0 Å, respectively), along with a weak diffraction at 18.5°. These peaks decrease a little in 2θ with increasing temperature, the peak near 22° being the most sensitive to this factor (it is located at 23.3° at ambient temperature, as shown in Figure 2). The spacings are similar to those observed for smectic E mesophases, in which the molecules within a layer are packed in a rectangular unit cell, with four molecules at its vertices and one in its center, forming an orthorhombic lattice. The corresponding cell parameters are $a = 8.0$ Å, $b = 5.4$ Å, $D = 4.8$ Å, $\phi = 68°$, and $S = 22$ Å, where a and b are the unit cell lengths, $2D$ is the diagonal length, ϕ is the interdiagonal angle, and S is the molecular area as given by $ab/2$; these values are comparable to those given elsewhere for S_E mesophases.[12,20] It is noteworthy that biphenyl mesogens frequently give rise to a smectic E mesophase.[12,21,22]

In summary, LC-4,6A is a thermotropic liquid crystal, characterized by a monotropic S_A mesophase at higher temperatures, in which the molecules are arranged in single layers, and a stable crystalline or highly ordered (possibly S_E) phase at lower temperatures, where the molecules are stacked orthogonally in bilayers. It is reasonable to suppose that the bilayers are composed of pairs of LC-4,6A molecules joined primarily in head-to-head fashion as H-bonded acid dimers. In the S_A mesophase, the bilayer order is lost, probably because the acid pairing has become dynamic and/or dissociated.

Thermal and Structural Analyses of LC-4,6A/P4VP Mixtures. When LC-4,6A is mixed with P4VP, the thermotropic behavior of the mesogen is significantly affected. The heating and cooling thermograms at 5 °C/min of LC-4,6A/P4VP mixtures at several acid/pyridine molar ratios are shown in Figure 3. It is observed that the thermal transitions for all of the mixtures are reduced in temperature compared to those for LC-4,6A. Furthermore, no focal conic texture on cooling from the isotropic phase is evident in any of the mixtures studied. Thus, the single transition in the 1.0 mixture, producing an unidentifiable, birefringent texture in the polarizing optical microscope on cooling, is likely to be an isotropic-to-ordered phase transition. This transition is shifted to lower temperatures in the 0.75 and 0.5 mixtures, where it is accompanied by a second, relatively broad transition at still lower temperatures. Below 0.4, only a single, broad transition is left, which tends to decrease somewhat with decrease in LC-4,6A content until the 0.2 molar ratio, where the transition is close to the limit of detection by DSC (see also Figure 5). At lower LC-4,6A contents, the small molecule and polymer appear to form a miscible, amorphous system. The enthalpy of the transitions (the total is given in the cases where there are two transitions), determined relative to the LC-4,6A molar content, is essentially constant in temperature for the mixtures of 0.5 and more (at about 28 kJ/mol LC-4,6A) but decreases rapidly to zero below that.

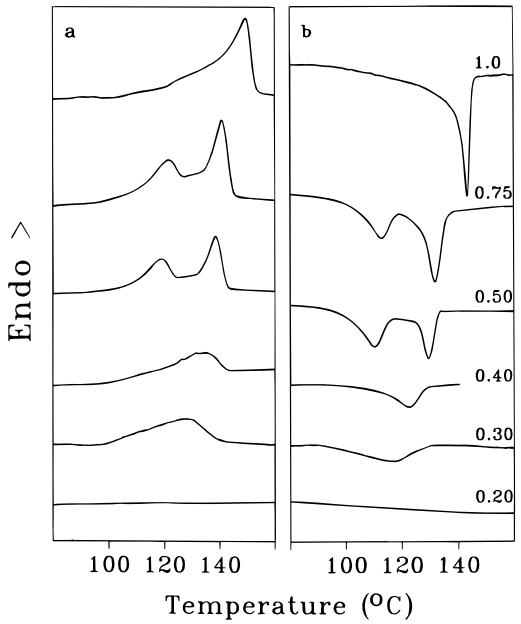

Figure 3. DSC thermograms [heating (a) and cooling (b) at 5 °C/min] of mixtures of LC-4,6A/P4VP at the acid/pyridine molar ratios indicated.

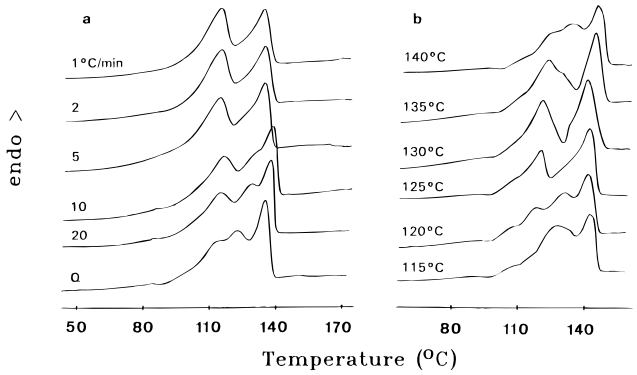

Figure 4. DSC heating thermograms (20 °C/min) of the LC-4,6A/P4VP mixture of 0.5 molar ratio: (a) after cooling the sample at the rates indicated (Q indicating a quench at a nominal rate of 320 °C/min), (b) after annealing the sample for 10 min at the temperatures indicated.

More detailed DSC investigations of the 0.5 mixture indicate that the transitions observed are subject to significant kinetic effects. In particular, the relative importance of the two transitions depends on thermal history, in particular the cooling rate, as shown in Figure 4 (where the thermograms were obtained at 20 °C/min). The slower the cooling rate, the more important the lower temperature transition. Faster cooling rates lead to more complex thermograms, with the appearance of what appears to be a third, intermediate temperature transition. It is possible that the latter is related to the single transition which appears in the mixtures with lower molar ratios of LC-4,6A. Annealing for 10 min at different temperatures between 115 and 140 °C (preceded by cooling at −5 °C/min from the melt to the annealing temperature, and followed by quenching from the annealing temperature to ambient temperature) leads only to more complex heating thermograms (as for the faster cooling rates). It is noteworthy that the minimum in these thermograms occurs at the annealing temperature for the samples that were annealed above the lower temperature transition.

(20) Doucet, J.; Levelut, A. M.; Lambert, M.; Liebert, L.; Strzelecki, L. *J. Phys. Colloq.* **1975**, *36*, C1−13.

(21) (a) Navarro-Rodriguez, D.; Guillon, D.; Skoulios, A.; Frère, Y.; Gramain, Ph. *Makromol. Chem.* **1992**, *193*, 3117. (b) Frère, Y.; Yang, F.; Gramain, Ph.; Guillon, D.; Skoulios, A. *Makromol. Chem.* **1988**, *189*, 419.

(22) (a) Demus, D.; Richter, L.; Ruerup, C. E.; Sackmann, H.; Schubert, H. *J. Phys. (Paris), Colloq.* **1975**, *1*, 349. (b) Dubois, J. C.; Zann, A. *J. Phys. (Paris), Colloq.* **1976**, *3*, 35.

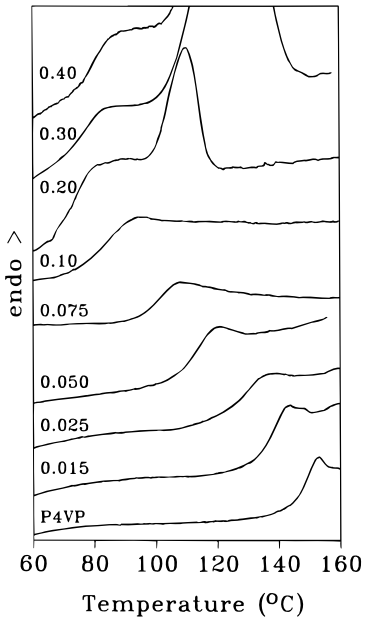

Figure 5. DSC heating thermograms (20 °C/min) of mixtures of LC-4,6A/P4VP at the acid/pyridine molar ratios indicated.

Another series of DSC thermograms, at a heating rate of 20 °C/min, was obtained for mixtures that include very low LC-4,6A contents in order to observe changes in the glass transition temperature (T_g) of P4VP with addition of the mesogen. These thermograms are shown in Figure 5. The T_g obviously decreases sharply from 147 °C to less than 80 °C with addition of LC-4,6A; this decrease is linear, at a rate of about 2.4 °C/wt % (7 °C/mol %) LC-4,6A added, up to a molar ratio of about 0.1 (about 25 wt % or 9 mol % LC-4,6A). When the first-order transitions appear (it is notable that a very small first-order transition is visible in the thermogram of the 0.2 mixture in Figure 5), the T_g remains essentially constant in temperature with further addition of LC-4,6A. This suggests that below a molar ratio of about 0.1, the LC-4,6A is dispersed throughout the polymer matrix and thus acts as a very effective plasticizer. Beyond a critical concentration, it is able to condense and form crystalline domains that are detectable by DSC above a molar ratio of about 0.2 (nearly 20 mol % LC-4,6A).

The plasticization of P4VP by small amounts of LC-4,6A was also observed by dynamic mechanical analysis, shown in Figure 6. The Young's storage modulus curves are displaced to lower temperatures with added LC-4,-6A; their slope in the glass transition region undergoes little change up to a molar ratio of about 0.1, where it appears to begin to decrease. The T_g's determined by the maximum of the loss tangent peaks parallel those observed by DSC. It is noteworthy that the intensities of the loss tangent peaks go through a maximum at a molar ratio of about 0.075.

It was observed from polarizing optical microscopy that, on cooling slowly from the isotropic phase, a birefringent texture grows in over several degrees, in feather-like fronts, resulting in a colorful, moss-like texture in the thicker areas and, at least for the mixtures of 0.5 molar ratio and below, some white, cloud-like textures and remaining homeotropic regions in thin areas. In the 0.5 mixture, the homeotropic regions fill in and the already birefringent regions

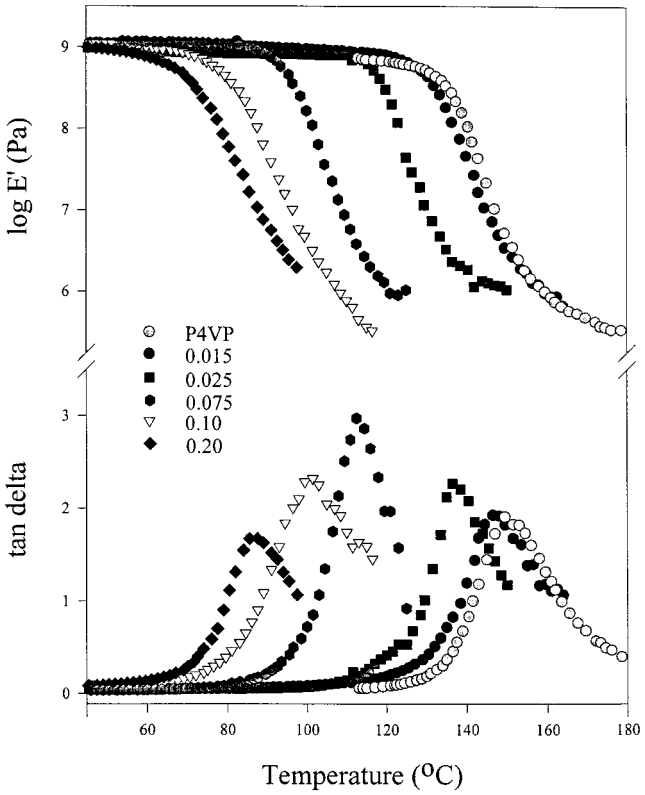

Figure 6. Dynamic Young's storage modulus and loss tangent (at 0.3 Hz) as a function of temperature for P4VP and for its mixtures with LC-4,6A at the acid/pyridine molar ratios indicated.

undergo a noticeable texture change during the lower temperature transition. This change is reversible on reheating into the intermediate phase. It was also observed that upon annealing in the intermediate phase, the birefringent regions tend to develop into more rounded textures. Furthermore, the sample is viscous in this phase and hardens only during the lower temperature transition. As the content of LC-4,6A in the mixtures is lowered, the birefringence observed becomes "diluted" and loses intensity.

X-ray diffractograms of various blends at ambient temperature are shown in Figure 7 [with the small angle region shown in detail in inset (a)]. The samples analyzed had been melted at 160 °C for about 10 min, and then cooled at a rate of 3 °C/min. For the mixtures with acid/pyridine molar ratios of 0.2 and more, the patterns are very similar to that of pure LC-4,6A and also to that of non-thermally-treated samples. All of the same peaks are present at the same positions. Evidently, the LC-4,6A molecules crystallize within the polymer matrix in the same form as they do when alone, namely, in orthogonal bilayers characterized by rectangular unit cells. This suggests that the LC-4,6A that has crystallized forms a separate phase from the polymer, with only minor (interfacial) interactions between the two components. Below 0.2, no crystalline structure can be detected in samples cooled from the melt (even after a week at ambient temperature), although, as shown in inset (b), a hint of structure is present in the profiles of the 0.1 and 0.05 (non-thermally-treated) powder samples. Only a broad amorphous peak centered near $2\theta = 20°$ remains present. This is altogether consistent with the DSC results.

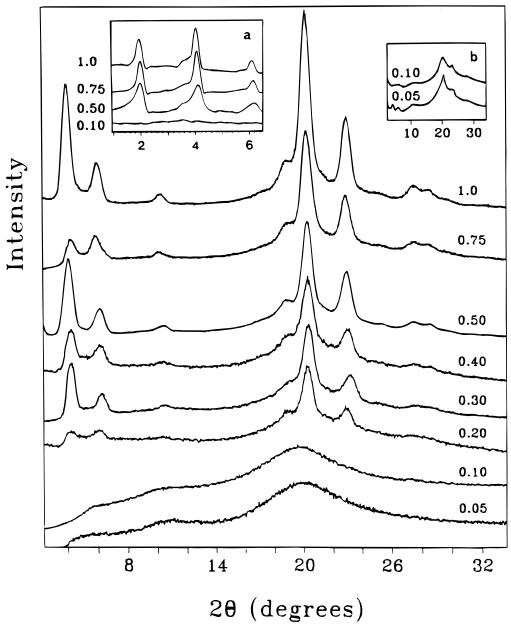

Figure 7. X-ray profiles of slowly-cooled samples of LC-4,-6A/P4VP mixtures at the acid/pyridine molar ratios indicated. Inset (a) gives the small-angle profiles obtained for the mixtures indicated. Inset (b) gives the profiles for some non-thermally-treated powder samples.

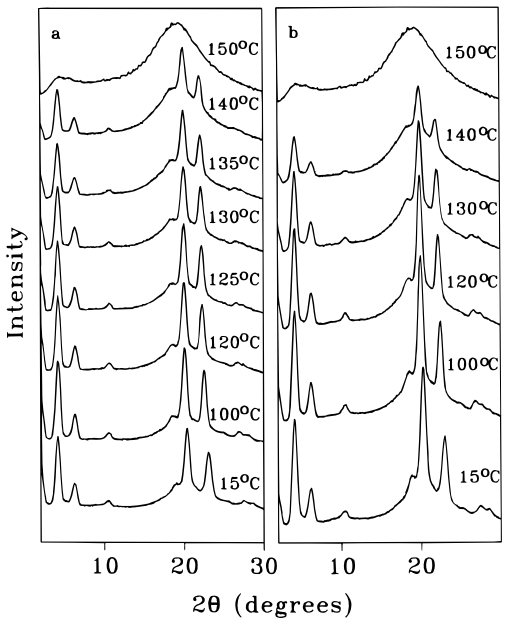

Figure 8. X-ray profiles of the 0.5 molar ratio LC-4,6A/P4VP mixture obtained at the temperatures indicated upon (a) heating and (b) cooling.

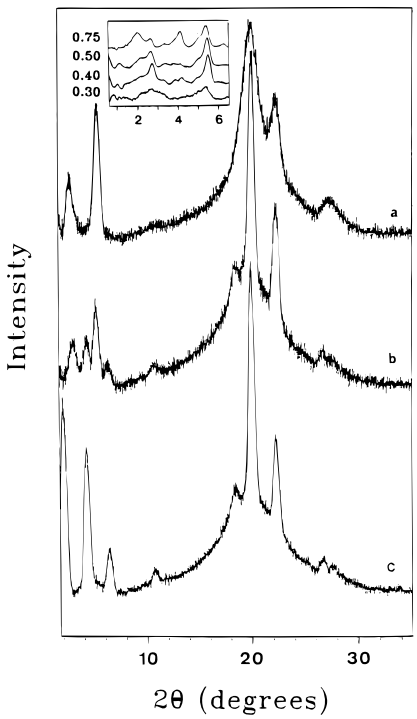

Figure 9. Unsmoothed X-ray profiles of the 0.5 molar ratio LC-4,6A/P4VP mixture obtained (a) at 50 °C after quenching from the melt, (b) after reheating the quenched sample to 125 °C, and (c) at 125 °C after slow cooling from the melt. The inset shows the small-angle profiles obtained for quenched mixtures of the molar ratios indicated.

As shown in Figure 8a for the 0.5 mixture, the evidence of crystalline structure at both wide and small angles gradually disappears, while the amorphous halo grows, upon heating in the temperature region corresponding to the two DSC transitions (about 110−145 °C). Thus, the phase between the two transitions in this blend corresponds not to a drastic change in structure but only to an increase in the amorphous component. At 150 °C, the sample is isotropic. Figure 8b shows that this is completely reversible. The gradual growth of the amorphous component with increasing temperature is consistent with the broadness of the DSC transitions. Indeed, isothermal X-ray profiles in the double transition range, including within the transitions, change little over time, as tested for up to 4 h.

It is of interest to note that structural change occurs in mixtures that are quenched from the melt. As shown in Figure 9, where the profiles of a quenched (a) and a slowly cooled (c) 0.5 mixture are compared, the two main peaks at wide angles remain present, although they are broadened somewhat. This indicates that the lateral packing of the molecules is basically unchanged. However, at small angles, the increase in the lowest angle peak positions indicates a significant decrease in lamellar spacing, to about 32 Å. Quenching obviously prevents formation of the bilayer structure obtained in slowly cooled samples. When the quenched sample is reheated into the intermediate phase [profile (b) of Figure 9], which is above the T_g of the sample, rearrangement slowly takes place and bilayer structure forms as shown by the reappearance of peaks corresponding to those of the slowly cooled sample.

The effect of quenching at small angles, shown in the inset of Figure 9, is similar for the mixtures of other molar ratios, although, with increasing LC-4,6A content, the simultaneous formation of a bilayer structure is increasingly difficult to suppress completely. It is also to be noted that the intensities of the diffraction peaks of the quenched samples are considerably lower than those of the slowly cooled samples, indicating less crystallinity in the former compared to the latter. This was supported by the observation of a recrystallization exotherm at about 115 °C in DSC heating thermograms (5 °C/min) of quenched samples of 0.3 and 0.4 molar ratios. Furthermore, although the detection of crystallinity by DSC in the 0.2 mixtures is difficult, molded samples of this composition that are slowly cooled are visually translucent whereas quenched ones are transparent.

The facts that the lamellar spacing in quenched samples is greater than single-layered LC-4,6A molecules and that the peaks are less well defined may indicate a frozen-in association with the polymer. Indeed, the length of an extended LC-4,6A molecule to which a 4VP unit is added is estimated to be about 30 Å, which is consistent with the experimental lamellar spacing of 32 Å. To probe this possibility in more detail, infrared analysis will be helpful.

Infrared Analysis. It was shown in our preliminary publication[17] that, in mixtures of LC-4,6A with P4VP, strong hydrogen-bonding occurs between the carboxylic acid and pyridine groups. This was illustrated by the decrease in intensity of a broad infrared band centered near 3100 cm^{-1} for LC-4,6A alone, attributed to the OH dimer stretch of hydrogen-bonded acid pairs, and the appearance of two new broad bands centered near 2500 and 1950 cm^{-1} which are attributed to strong H-bonding between carboxylic acid and pyridine. These bands are visible for molar ratios of acid to pyridine up to at least 2.0. Similar results were obtained by other researchers for systems involving the same two interacting groups.[1,23] Figure 10 compares the spectra, in the high-wavenumber region, of a slowly cooled and a melt-quenched mixture of 0.5 molar ratio, along with the spectra of the pure components. It is immediately striking that the two absorption bands near 2500 and 1950 cm^{-1}, present in both mixtures, are significantly more intense in the quenched sample than in the slowly cooled sample. The broad band around 3100 cm^{-1} also appears to be decreased more in the former than in the latter. This is indicative that, although there is acid−pyridine H-bonding in both mixtures, it is present to a considerably greater extent in the quenched samples than in the slowly cooled samples. Apparently, association between P4VP and LC-4,6A is much more favored in the melt, from where it can be frozen in by quenching.

Two other spectral regions supporting this analysis are that between 1700 and 1750 cm^{-1}, which involves the carbonyl stretch, and that around 1000 cm^{-1}, which involves a pyridine ring mode. The usefulness of these regions has been highlighted previously by Lee et al.[23] for blends of poly(ethylene-*co*-methacrylic acid) with a copolymer of styrene and 2-vinylpyridine. Changes noted in the region of another pyridine absorption band near 1600 cm^{-1} are obscured in our case by the presence of a phenyl ring absorption by the LC-4,6A (as can be observed in Figure 11).

The evolution with composition that is observed in the carbonyl region from 1650 to 1750 cm^{-1} and in the pyridine ring mode region from 980 to 1020 cm^{-1}, for a sample cooled slowly from the melt, is illustrated in Figure 11.[24] For pure LC-4,6A, the carbonyl region is dominated by a strong band at 1695 cm^{-1}, attributed to H-bonded carbonyl, indicating that dimerized acid groups are the predominant species in pure LC-4,6A; the weaker band at 1733 cm^{-1}, attributed to free carbonyl, reflects the presence of a certain amount of unassociated acid groups.[23] As P4VP is added to LC-4,6A, a third band, at 1713 cm^{-1}, develops at the expense of the other two and is the dominant band for mixtures of 0.2 molar ratio and less. Lee et al.[23] attributed this band to free carbonyl groups whose absorption is shifted to lower frequencies because of polar interactions with adjacent pyridine groups. Thus, it reflects the existence of hydrogen-bonding between the acid and pyridine groups; these interactions liberate carbonyl groups from hydrogen bonding in acid dimers but juxtapose them with pyridine groups.

Similarly, despite the presence of two LC-4,6A absorptions at around 1000 cm^{-1}, it is obvious that the ring-mode absorption of nonassociated pyridine groups at 994 cm^{-1} becomes partly replaced by a new absorption at 1012 cm^{-1} that is attributed to pyridine groups associated with acid moieties.[23] This is especially

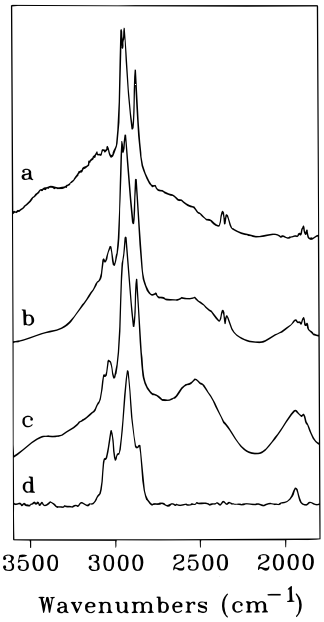

Figure 10. Infrared spectra of (a) LC-4,6A, (b) slowly-cooled 0.5 LC-4,6A/P4VP, (c) quenched 0.5 LC-4,6A/P4VP, and (d) P4VP.

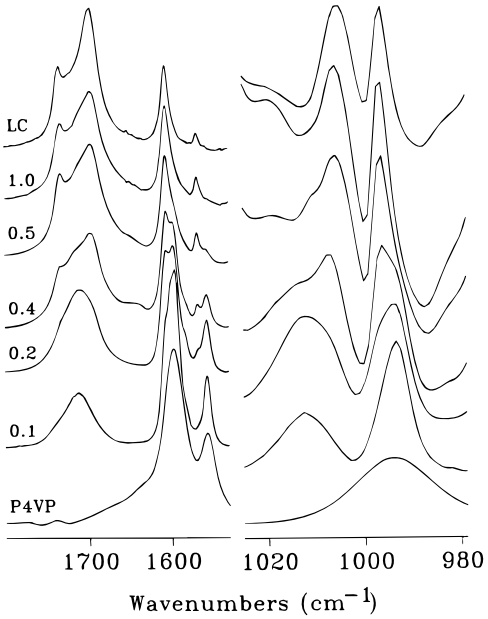

Figure 11. Infrared spectra of slowly cooled samples of pure LC-4,6A and P4VP and their mixtures at the acid/pyridine molar ratios indicated.

(23) Lee, J. Y.; Painter, P. C.; Coleman, M. M. *Macromolecules* **1988**, *21*, 954.

(24) The spectra presented in ref 17b were of samples that had been taken directly out of a vacuum oven heated to roughly 140 °C; thus, those samples had been inadvertently quenched, and their spectra resemble those of the quenched samples of the present study.

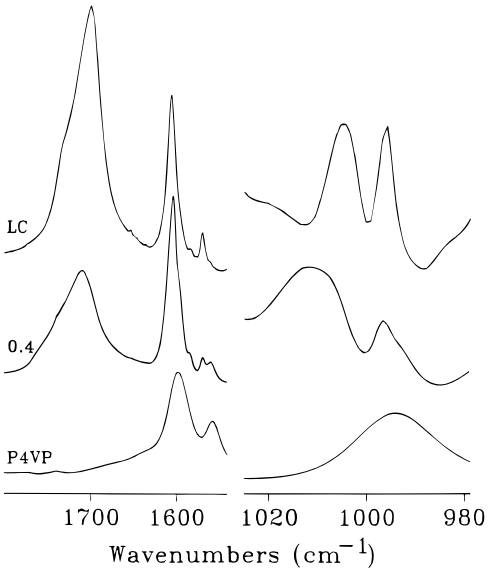

Figure 12. Infrared spectra of quenched samples of pure LC-4,6A and the 0.4 LC-4,6A/P4VP mixture; a spectrum of pure P4VP is included for comparison.

evident for acid/pyridine molar ratios below 0.5, where the LC-4,6A absorptions are less important.

The spectra, in the same two regions, of samples quenched from the melt are shown in Figure 12. It can be observed that the free and dimer carbonyl bands in pure LC-4,6A are somewhat less well defined in quenched samples than in slowly cooled samples, probably reflecting greater variation in the local environments around the carbonyl groups, due to a less perfect alignment of hydrogen-bonded pairs in lamellar layers. However, what is the most striking is the much greater evidence of acid−pyridine hydrogen bonding in the quenched mixtures compared to the slowly cooled mixtures. This is illustrated in the spectra shown of the 0.4 mixture, where it can be observed that the 1713 cm^{-1} band is the dominant band in the quenched sample (just as it is in the slowly cooled 0.1 sample shown) and the band at 1012 cm^{-1} is much more intense (at the expense of the 994 cm^{-1} band) in the quenched sample than in the slowly cooled sample. It can also be observed that the pyridine band at 1596 cm^{-1} relative to the band at 1605 cm^{-1} (which includes both the LC-4,6A phenyl band and, presumably, the hydrogen-bonded pyridine band[23] corresponding to the nonassociated band at 1596 cm^{-1}) is less intense in the quenched (Figure 12) than in the slowly cooled (Figure 11) mixture, another sign of increased acid−pyridine hydrogen bonding in the former.

Finally, a series of spectra were taken of 0.5 mixtures quenched from various temperatures that are within the range of the first-order transitions (the samples, prepared from $CHCl_3$ in this case, were cooled slowly to these temperatures from the melt), in an attempt to obtain information about the evolution of the extent of hydrogen bonding. The spectral regions of interest are shown in Figure 13. Each of these spectral regions, whether shown by the decrease in intensity of the 2500/1950 cm^{-1} pair, the 1713, 1605, or 1012 cm^{-1} bands, or the increase in the 1733, 1695, 1595, or 994 cm^{-1} bands, indicates that there is a significant decrease in acid−pyridine hydrogen bonding below the higher temperature transition. This is consistent with the X-ray data which show that the bilayer structure forms already in the intermediate phase.

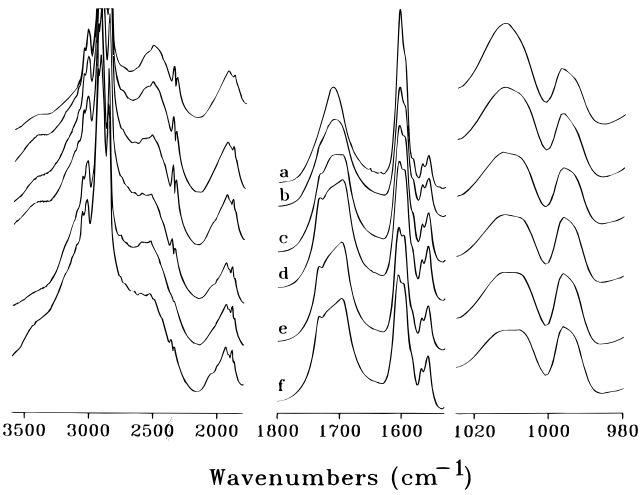

Figure 13. Infrared spectra of the 0.5 LC-4,6A/P4VP mixture quenched from various temperatures: (a) 165, (b) 130, (c) 125, (d) 120, (e) 115, and (f) 110 °C.

Discussion and Conclusions

The picture that emerges of the functionalized mesogen/polymer system described above can be summarized as follows. At low LC-4,6A contents, miscible amorphous blends are formed and the mesogen simply acts as a stronger plasticizer. It is undoubtedly the hydrogen-bonding interactions between the acid group of LC-4,6A and the pyridine groups in the polymer that cause the mesogen to be dispersed throughout the polymer matrix. Beyond a certain concentration of LC-4,6A, however, acid−pyridine interactions are no longer thermodynamically favored; rather, the mesogen molecules begin to coalesce and form highly ordered or crystalline domains at lower temperatures. This is detectable by DSC and X-ray diffraction at a mesogen/repeat unit (acid/pyridine) molar ratio of about 0.2. At this point, no further plasticization takes place, and the system can be considered to have become immiscible. In other words, LC-4,6A has a solubility limit in P4VP. On the other hand, above the melting point of the mesogen, miscibility of the two components is considerably enhanced due to the acid−pyridine interactions. It is therefore possible to freeze in the interactions and have significant amounts of P4VP incorporated into the ordered domains by quenching the samples from the melt (as shown both by infrared spectroscopy and by the change in the X-ray lamellar spacing indicating a bilayer structure to one apparently indicating a single-layered structure that includes a 4VP unit); this, of course, leads to a decreased amount of crystalline or highly ordered phase as well as to the domains that do form being more poorly ordered (as shown by the decrease in intensity and by the greater coarseness, respectively, of the X-ray profiles of the quenched samples compared to the slowly cooled samples).

The plasticization of the polymer that is observed at low LC-4,6A concentrations is typical of what is generally observed in miscible blends of polymers and small molecules (external plasticization) as well as in polymers whose backbones are partially substituted by flexible side chains such as *n*-alkyl substituents (internal plasticization). The strong acid-pyridine hydrogen-bonding interactions in the LC-4,6A/P4VP system can be thought of as leading to a kind of plasticization

intermediate to external and internal, in that the interactions cause the non-covalently-bound LC-4,6A molecules to be positioned (at least momentarily) like covalently attached side chains. Similar effects were observed by us for mixtures of poly(ethyl acrylate) with 4-decylaniline, where H-bonding interactions are thought to take place between the ester groups of the polymer and the amine terminal moiety of the small molecule.[25]

Phenomena resembling those in our LC-4,6A/P4VP system were reported by Belfiore et al. for mixtures of zinc laurate with P4VP,[26] as well as for mixtures of *p*-(pentyloxy)cinnamic acid (which, in neat form, is liquid crystalline) with bisphenol-A polycarbonate.[27] In the former case, where coordination complexes are formed between the Zn salt and pyridine units, the T_g of the P4VP is decreased at a rate of about 4−5 °C/mol % Zn laurate to nearly 70 °C and then remains constant above about 20 mol % Zn laurate; a depressed crystalline transition appears in DSC by 40 mol % Zn laurate content, reaching its neat−state value near 60 mol % Zn laurate content. It was concluded from this data and from high-resolution carbon-13 solid-state NMR analysis that these mixtures are composed of an amorphous polymer-rich phase, which gives rise to the T_g, and a small-molecule-rich phase, which is the source of the first-order transition.

In comparing the P4VP/LC-4,6A and the P4VP/Zn laurate systems at a particular point in the linear region of T_g depression, 8 mol %, it is noted that the decrease per axial atom (counting three axial atoms for each phenyl moiety) of the small molecule is roughly 3 °C in both systems. This is comparable to 2.5 °C/carbon atom observed for stoichiometric blends of linear alkyl amines with polystyrene sulfonated to 8 mol %, where proton transfer from the amine to sulfonic acid takes place leading to ion−ion interactions,[28] and to 2.4 °C/carbon atom observed for copolymers of styrene and 7 mol % 4-vinylpyridine quaternized with iodoalkanes (thus, with the side chains covalently attached to the polymer backbone).[29] It is also noteworthy that the maximum decrease in T_g and the solubility limit of the small molecules in P4VP appears to be somewhat greater in the P4VP/Zn laurate system (about 70 °C, 30−35 mol % Zn laurate) than in the P4VP/LC-4,6A system (75−80 °C, about 20 mol % LC-4,6A), even though the Zn laurate molecule is shorter in axial length than the LC-4,6A molecule. This may be related to the type of interactions involved (coordination vs H-bonding), to the greater propensity (thermodynamic driving force) for crystallization of the biphenyl-containing alkyl chain compared to the linear alkyl chain, and/or to the greater rigidity of the biphenyl segment in LC-4,6A.

At higher LC-4,6A concentrations, where first-order transitions appear, we can consider that we have a two-phase system (as for the P4VP/Zn laurate mixtures) composed of the (plasticized) P4VP-rich phase and a LC-4,6A (or LC-4,6A-rich) phase. The facts that the transitions in the mixtures occur at lower temperatures and over a broader range than that of neat LC-4,6A and that the monotropic S_A mesophase is no longer present in the mixtures (in the concentration range studied) are indications that the second phase may include a minor amount of polymer and is therefore LC-4,6A-rich. On the other hand, these facts may also simply be a consequence of the increased acid-pyridine interactions in the melt that overrides the appearance of the S_A mesophase and that retards solidification as well as perturbs the sizes and order of the domains (the latter effects are similar to what is frequently observed in melt-miscible polymer blends involving a semicrystalline component[30]). Certainly, whatever P4VP may be incorporated into the ordered phase is small enough that the overall structure of these domains is the same as that of pure LC-4,6A, namely, characterized by acid dimers, although with some loss of definition. As mentioned above, a large amount of polymer can be incorporated in the solid phase by quenching mixtures from the melt, such that the lamellar spacing of the ordered domains is completely changed.

The appearance of two transitions in some of the mixtures cannot be explained with certainty at this point. Certainly, the experimental data indicate ordering into the same molecular structure (bilayer lamellar phase) in two stages on cooling. One possibility is that there are two concentrations of LC-4,6A-rich phases or two significantly different domain sizes and/or degrees of imperfection. This may be a reflection of the extent of association of the two components in the melt phase. The higher the LC-4,6A content, the lesser the proportion of LC-4,6A molecules associated with the polymer in that phase. When there is a sufficient number of unassociated LC-4,6A molecules present locally, those that are H-bonded to the polymer can easily rearrange during the ordering process into H-bonded dimers with neighboring LC-4,6A molecules that are already unassociated. In other words, at high LC-4,6A contents, a single ordering process takes place that is controlled by the presence of polymer-unassociated LC-4,6A. For lower LC-4,6A contents, where the degree of association with polymer in the melt is higher, the ordering process may be controlled by the associated LC-4,6A, which must rearrange from H-bonding with the polymer into H-bonded dimers with itself, not necessarily in its immediate neighborhood; possibly, this process also involves conformational rearrangement of P4VP segments that may remain associated with some of the ordered LC-4,6A. This process takes place then at lower temperatures. It is possible that, at intermediate LC-4,6A contents, there are local domains where there is a higher proportion of unassociated LC-4,6A, and where ordering first takes place on cooling from the melt, whereas the rest, with a lower proportion of unassociated LC-4,6A, solidifies into ordered domains at a lower temperature. This would actually give rise to a mixed-phase morphology of microdomains. The fact that the birefringent regions that develop at the first transition, on cooling the 0.5 mixture as observed in the polarizing optical microscope, undergo a noticeable texture change

(25) Tong, X.; Bazuin, C. G. *J. Polym. Sci., Part B: Polym. Phys.* **1992**, *30*, 389.
(26) Belfiore, L. A.; Pires, A. T. N.; Wang, Y.; Graham, H.; Ueda, E. *Macromolecules* **1992**, *25*, 1411.
(27) Patwardhan, A. A.; Belfiore, L. A. *Polym. Eng. Sci.* **1988**, *28*, 916.
(28) Smith, P.; Eisenberg, A. *J. Polym. Sci., Part B: Polym. Phys.* **1988**, *26*, 569.
(29) Wollman, D.; Gauthier, S.; Eisenberg, A. *Polym. Eng. Sci.* **1986**, *26*, 1451.
(30) MacKnight, W. J.; Karasz, F. E.; Fried, J. R. In *Polymer Blends*; Paul, D. R., Newman, S., Eds.; Academic Press: New York, 1978; Vol. 1, Chapter 5.

during the lower temperature transition, is indicative of the small-scale nature of the domains proposed. The above picture is consistent with the greater amorphous component present in the X-ray diffraction profile of the intermediate phase (compared to the lower temperature phase) as well as with the shearable nature of this phase and the effects of annealing in this phase. It is also consistent with the decrease in acid−pyridine association observed from the infrared spectra of samples quenched from this phase compared to the melt phase.

Further studies of these systems, using variable-temperature solid-state NMR and infrared spectroscopies as well as rheological analyses in the melt, are in progress.

Acknowledgment is made to the donors of the Petroleum Research Fund, administered by the American Chemical Society, for partial support of this research. We are also grateful to NSERC (Canada) and FCAR (Québec) for additional financial support. Prof. Antoine Skoulios and Mr. Rachid Seghrouchni of l'Institut de Physique et Chimie des Matériaux de Strasbourg, in France, are sincerely thanked for DSC, microscopy, and X-ray measurements on LC-4,6A that helped set us on track at a time when our X-ray facilities were not yet well adapted to thermal analyses; we also thank Prof. Skoulios for helpful discussions.

CM950240R